Cumhuriyet Sci. J., 45(4) (2024) 750-755
DOI: https://doi.org/10.17776/csj.1534439

Cumhuriyet Science Journal

| csj.cumhuriyet.edu.tr | Founded: 2002 ISSN: 2587-2680 e-ISSN: 2587-246X Publisher: Sivas Cumhuriyet University

Modeling the Effect of Heat Distribution in Photothermal Therapy by Using Computational Fluid Dynamics (CFD)

Mesude Avci [1,a,*]

[1] *Department of Chemical Engineering, Sivas Cumhuriyet University, Sivas, Türkiye*
**Corresponding author*

Research Article

History
Received: 16/08/2024
Accepted: 14/12/2024

ABSTRACT

Cancer is a mortal disorder around the world, and according to the World Health Organization (WHO), it is a leading cause of death, causing nearly 10 million deaths in 2020. It is commonly treated by chemotherapy, radiotherapy, and surgery. However, the undesirable effects of these treatments encouraged clinicians to find better therapies, such as photothermal therapy (PTT). PTT has been commonly used for being less harmful to the healthy tissues near the cancer cells. However, it is necessary to know that the heat distribution is suitable and that the surrounding tissue is not overheated. This work uses Computational Fluid Dynamics (CFD) to model the cancer cell and the healthy tissue around it as a 3D model using ICEM CFD, a pre-processing program of Ansys Fluent 18.2. It is found that wall shear stress is high, up to 4600 Pa in the top parts of the cell, and lower in others. The highest pressure on the cancer cell goes up to 36000 Pa in the lower parts of the cell. The results of this work could guide researchers in optimizing the photothermal therapy of cancer cells, and the modeling approach could be applied to investigate alternative therapies.

Keywords: Cancer cell, Photothermal therapy, Computational Fluid Dynamics, Heat distribution, Modeling.

[a] *mesude@cumhuriyet.edu.tr* *https://orcid.org/0000-0001-8211-7779*

Introduction

Cancer is an uncontrolled failure of abnormal cells that can attack and deteriorate normal bodily tissue. In addition, cancer also expands all over the body in an unpredictable process. According to the World Health Organization (WHO), cancer is a leading cause of death, causing nearly 20 million new cancer cases and 09.7 million deaths in 2022. Moreover, the determined number of people who were alive within 5 years following a cancer diagnosis was 53.5 million. About 1 in 5 people develop cancer in their lifetime [1,2]. However, advancements in traditional cancer therapies, such as photothermal therapy, have provided a continued decrease in cancer death rates since the early 1990s [2], [3]. Cancer is commonly cured by chemotherapy, radiotherapy, and surgery. Nevertheless, these therapies may have undesirable effects on the body, such as damaging healthy cells, injuring the patient's immune system, and causing several harmful side effects. As a result of these inefficiencies, new effective therapies to destroy cancer cells without damaging healthy cells have been commonly developed [4-6]. Among other new therapies, there has been much interest in cancer photothermal therapy because of its minimal adverse effects on the healthy cells around the cancer cells.

Photothermal therapy (PTT) is a well-known method for cancer therapy that uses high temperatures generated from optical energy to activate cancer cell burn death [7–11]. Considering other therapies, such as radiotherapy and chemotherapy, PTT cancer treatment is very selective and minimally invasive because the healing effect of PTT cancer treatment occurs only at the sick cell site without harming normal tissues [12]. Besides being an effective therapy on its own, hyperthermia has also been well applied and showed a reduction of tumor size with other tumor treatment methods such as chemotherapy and radiation with the [13-16]. Coleman et al. [17] worked on regional hyperthermia where tumor cell temperature is increased above 42°C for a couple of hours.

When heating cancer cells, it is essential to know that the healthy tissue near them is not harmed. Due to hyperthermia, the surrounding tissue and muscles are also exposed to heat. Heat distribution affects the PTT since too much heat can damage cancer cells and human tissue. Therefore, it is essential to examine the suitable heat distribution and the effect of heat in PTT so that hyperthermia will burn the cancer cells without overheating and damaging the surrounding tissues [18].

This study is different from the literature since it addresses the direct effect of temperature both on the cancer cell and also on the healthy tissue around the cancer cell. This study also carefully considers the change of different parameters, such as wall shear stress and pressure in PTT. Moreover, the temperature effect is comprehensively examined by modeling different temperature ranges for the cancer cell and the healthy tissue around it. This study examines the heat effect of PTT on the cancer cell. It evaluates the heat distribution on the cancer cell and surrounding tissue. It also shows the impact of temperature increase, pressure, and wall

shear stress on the cancer cell. Furthermore, the healthy tissue near the cancer cell is also investigated.

Methods

Model Development and Computational Mesh Generation

A cancer cell and healthy tissues around the cancer cell are modeled and meshed as a 3D model using ICEM CFD, a preprocessing program of Ansys Fluent 18.2 (a finite volume approach). A cancer cell is defined as a spherical particle (to reduce the computational time) with a 5 mm diameter, which is not the actual size, and the healthy tissue around the cancer cell is modeled as a cube with a side length of 10 cm. One assumption is that the cancer cell is modeled as a spherical particle. This assumption is made to simplify the simulations. This assumption might not change the results since this study considers the heat effect on the cancer cell, and the cancer cell shape is not very different than the spherical shape. Another assumption, which is using water near the cancer cell, does not change the results since the density and viscosity values of plasma are close to the values of water. The cancer cell size is not the actual size of a human cell, but this work focuses on the heat transfer from the cancer cell and the changes in the healthy tissues around the cancer cell during photothermal therapy. The illustration of the 3D model of the cancer cell and the healthy tissue is represented in Figure 1.

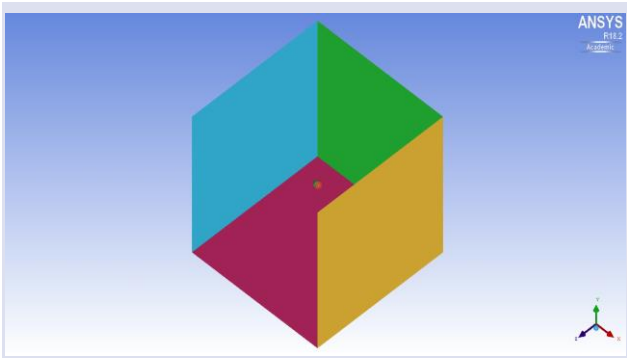

(a)

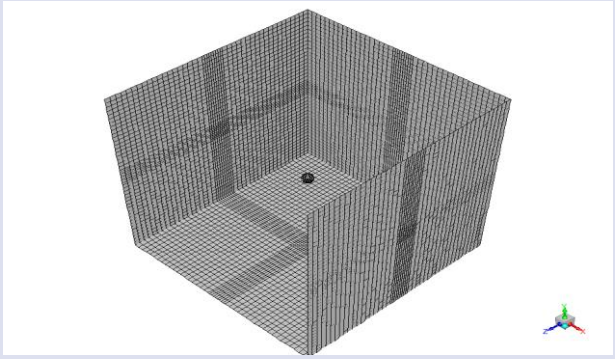

(b)

Figure 1. (a) 3D computational model, (b) Meshing of the model. In both figures, the cancer cell is shown as a spherical particle in the middle, and the healthy tissue around the cancer cell is shown as a cube around the sphere.

In Figure 1, the top and one side of the box are not displayed to increase the visibility of the cancer cell inside the box. Once geometric shapes have been produced, meshing proceeded with the formation of hexahedral elements throughout the entire geometry. After the meshes are constructed, the flow geometries are imported into Fluent to solve the incompressible Navier-Stokes equations. Grid independence of the models is tested by refining the temperature at multiple cross-sectional cuts between a more and less refined simulation solution was <3%. The model has approximately 105 524 cells and 112 520 nodes. Grid-independent analysis for temperature is shown in Figure 2.

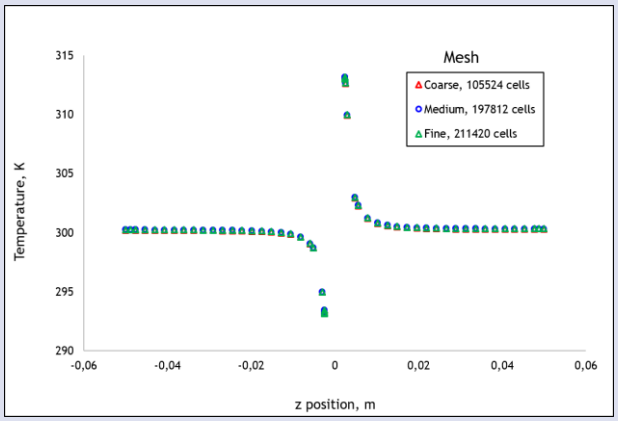

Figure 2. Grid independence analysis for the model.

It can be seen from Figure 2 that temperature values are independent of different mesh sizes. Since different grid sizes are independent of the results, the medium mesh size with 197812 cells is chosen for all simulations for modeling the cancer cell.

Flow Simulation

The finite volume-based Fluent simulator is used to model the cancer cells and healthy tissues and solve the governing equations in the flow field. The specified boundary conditions for the simulations include; the wall boundary conditions for the cancer cell and wall boundary conditions for the sides of the cube, which are representative of the healthy cell, with no-slip boundary conditions on the walls. In Ansys Fluent, the second-order upwind scheme is applied to discretize the momentum and the energy equations, with the SIMPLE algorithm utilized for pressure-velocity coupling. The time parameters for the simulations are specified as the steady state condition. In the case of heat required in photothermal therapy, there is one infrared heat source. Heating the cancer cell is represented by modeling the cell as hot on one side and colder on the other. Different temperatures are specified for the hot side of the cancer cell to define the more prolonged heating and, therefore, to show better the effect of heat transfer to healthy tissues around the sick cell. The current temperatures used in the model are 20°C for the cold part of the cancer cell and 40°C for the hot side. Different variations of the temperatures are also tried, such as the hot part of the cell being increased up to 80°C to have a bigger difference

between the cold and the hot part. Since similar results are obtained, only 20°C for the cold side and 40°C for the hot side of the cell configuration are presented here for simplicity. The simplified model setup schematics are shown in Figure 3.

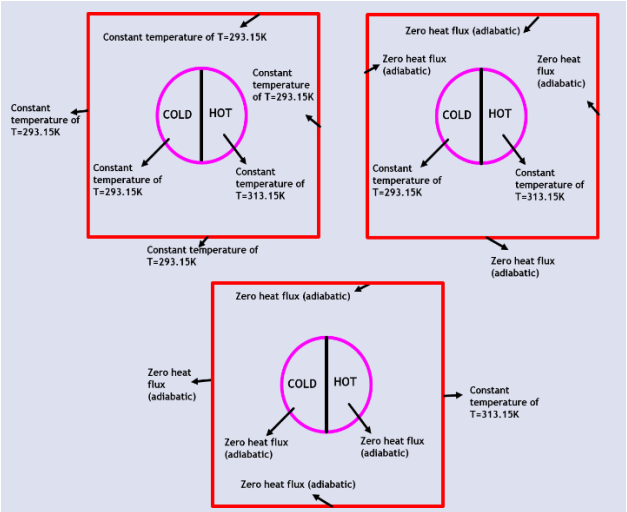

Figure 3. The simplified model setup schematics of the cancer cell and the healthy tissue around it.

The model parameters for the plasma of healthy tissue, such as density, viscosity, specific heat, and thermal conductivity, are specified depending on temperature. For simplicity, the healthy tissue plasma is considered water, and each particular parameter is defined for a specific equation, which depends on temperature.

Model parameters for the flow simulation

The density, specific heat, thermal conductivity, and dynamic viscosity data of water at different temperatures are taken from the literature [19]–[23]. Regression analysis determines the best fit for these parameters as a temperature function. The resulting formulas are shown in Equations 1 to 4, and the regression plots are represented in Figure 4.

$$\rho = -0.0046T^2 + 2.5183T + 656.86 \quad (1)$$
$$c_p = -0.0005T^3 + 0.5059T^2 - 160.9T + 21204 \quad (2)$$
$$k = -9E-06T^2 + 0.0068T - 0.6455 \quad (3)$$
$$\mu = 0.3664T^2 - 242.85T + 40733 \quad (4)$$

where ρ is density, c_p is the specific heat, k is the thermal conductivity, μ is the dynamic viscosity, and T is the temperature.

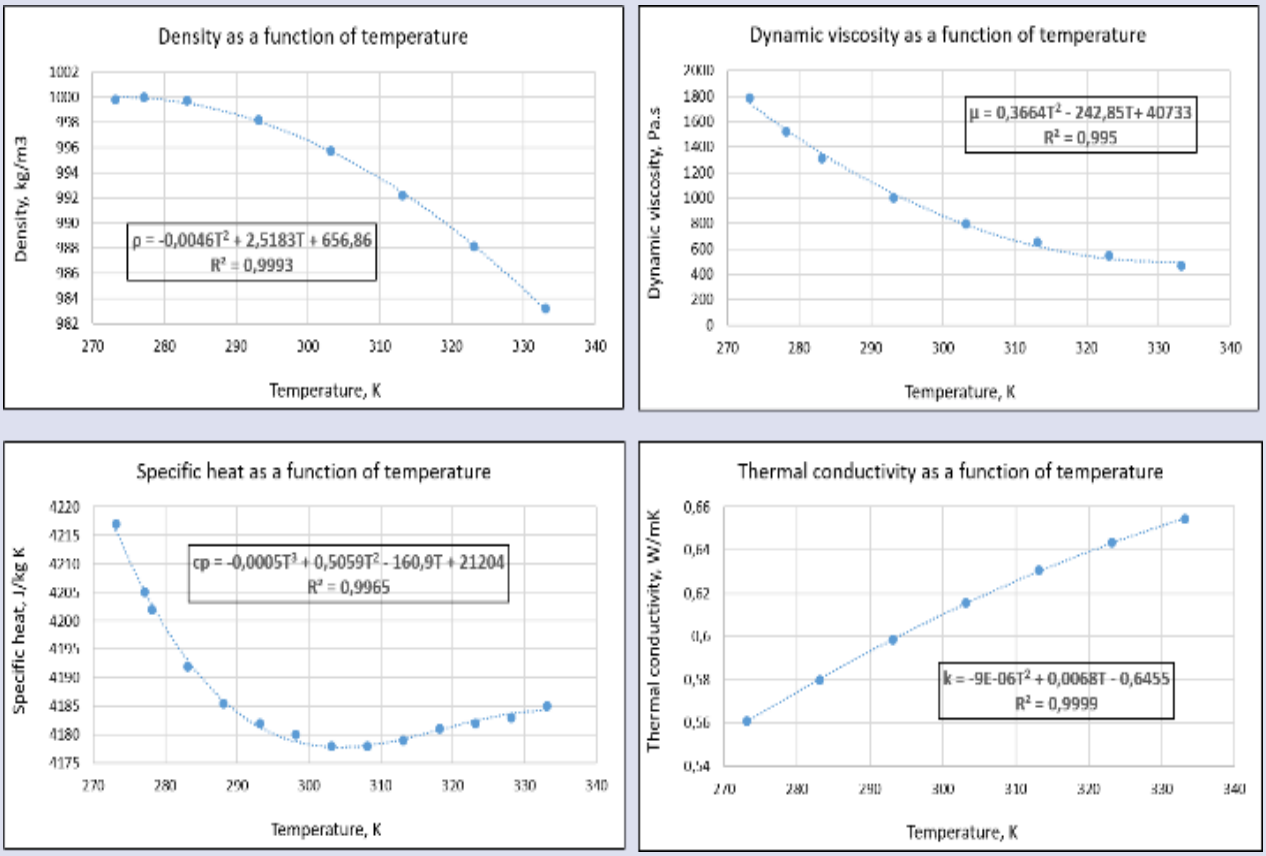

Figure 4. Top left: The density of water as a function of temperature; top right: The dynamic viscosity of water as a function of temperature; bottom left: Specific heat of the water as a function of temperature; and the bottom right: the thermal conductivity of water as a function of temperature.

Results and Discussion

Effect of Temperature on Cancer Cells

Photothermal therapy is represented when the cancer cell is heated on one side and cooler on the other. The highest temperature is 312 K, while the coldest temperature is 294 K. Figure 5 shows the temperature contours of the cancer cell.

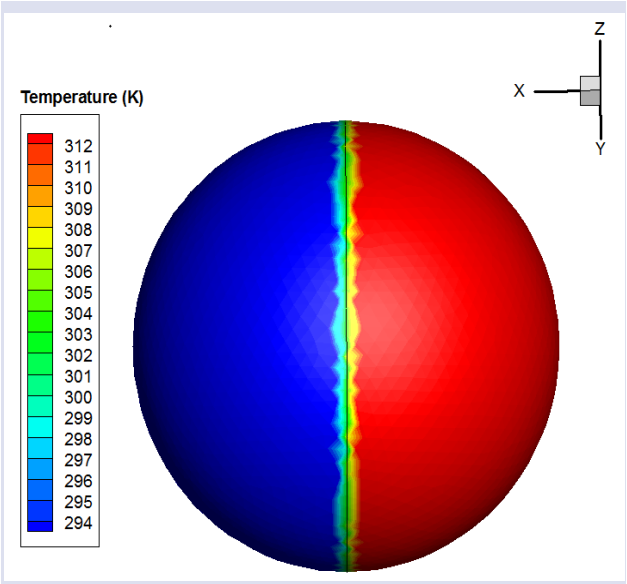

Figure 5. Temperature contours on the cancer cell.

As shown in Figure 5, the side of the cancer cell that is heated by an infrared heat source has a high temperature. After the heating effect on cancer cells, it is important to observe their behavior. The error analysis shows that the model shows adequate correctness, which can also be seen in the R^2 values in Figure 4. The determined R^2 values are 0.9993 for the density equation, 0.995 for the dynamic viscosity equation, 0.9965 for the specific heat distribution, and 0.9999 for the thermal conductivity distribution. Therefore, more parameters of the cancer cell are observed. The change of the wall shear stress on the cancer cell is shown in Figure 6.

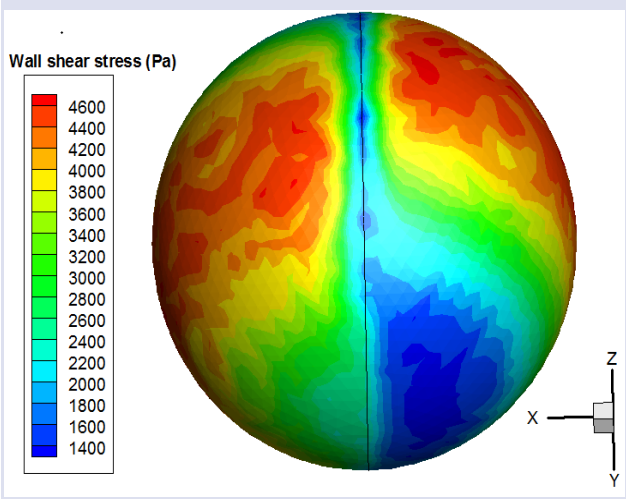

Figure 6. Wall shear stress contours on the cancer cell.

Figure 6 shows the wall shear stress values distribution on the cancer cell. Wall shear stress is high, up to 4600 Pa in the top parts of the cell. The value of the wall shear stress is lower in the lower parts. The lowest value is 1400 Pa. Pressure values are also determined on the cancer cell and are illustrated in Figure 6.

It is essential to analyze the wall shear stress profile on a cancer cell because it will affect the structure and the behavior of cancer cells to the endothelial cells [24]. The wall shear stress has been found to be a key component for a cancer cell and the endothelial cell in the vicinity of the cancer cell in the critical process in the metastatic scenario for affecting the cancer cell stiffness and adhesion of cancer cells to microvasculature [24].

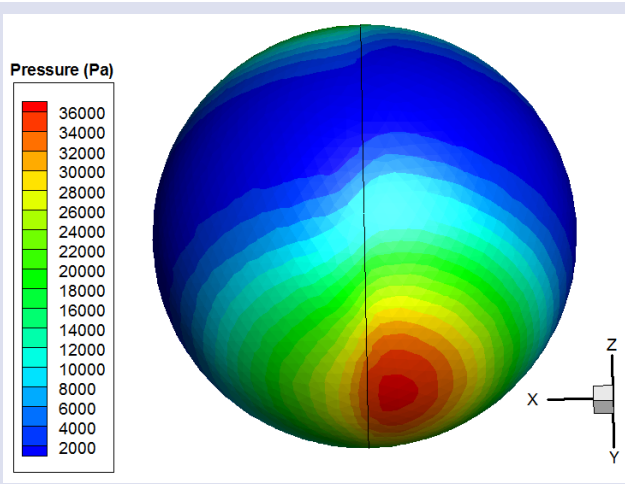

Figure 7. Pressure contours on the cancer cell.

Figure 7 shows the distribution of the pressure values stress on the cancer cell. The highest pressure on the cancer cell goes up to 36000 Pa in the lower parts of the cell. The pressure value is lower on the top parts of the cell. The lowest value is 2000 Pa.

High-pressure values on cancer cells could stimulate their proliferation by affecting their stiffness compared to surrounding cells [25]–[28]. Pressure changes in cancer cells have been found to affect their peripheries, perfusion, and the delivery of chemotherapy. The high-pressure values will also influence the movement of cancer cells, if there are any [25]–[28].

Effect of Temperature on Healthy Tissues in the Vicinity of Cancer Cells

As discussed above, the healthy tissue near the cancer is modeled using a box around the cancer cell. In addition, the heat change around the cancer cell is scrutinized by adding more planes inside the box; some are very close to the cancer cell, and some are attached to the cancer cell. Also, several lines cut through the cancer cell from one side of the box to the other are created for a more detailed analysis. The plane analyzed here cuts the cancer cell at the center, which is presented in Figure 8A. The illustration of the plane attached to the cancer cell and the line are illustrated in Figure 8.

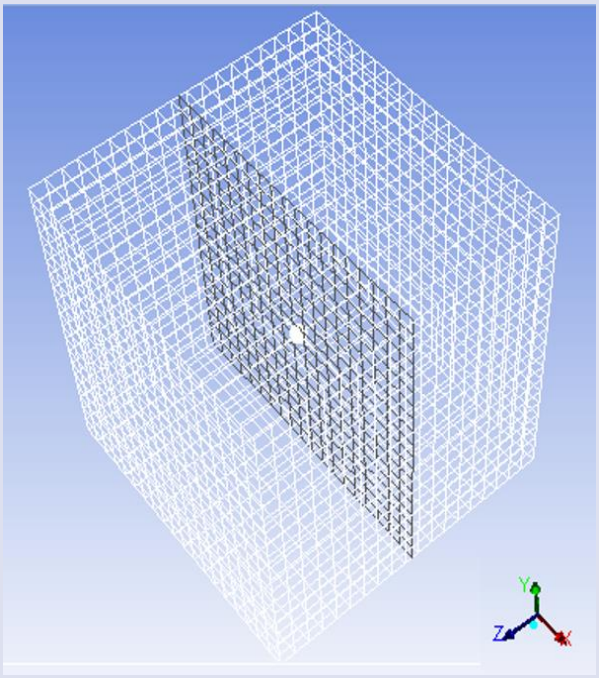

(a)

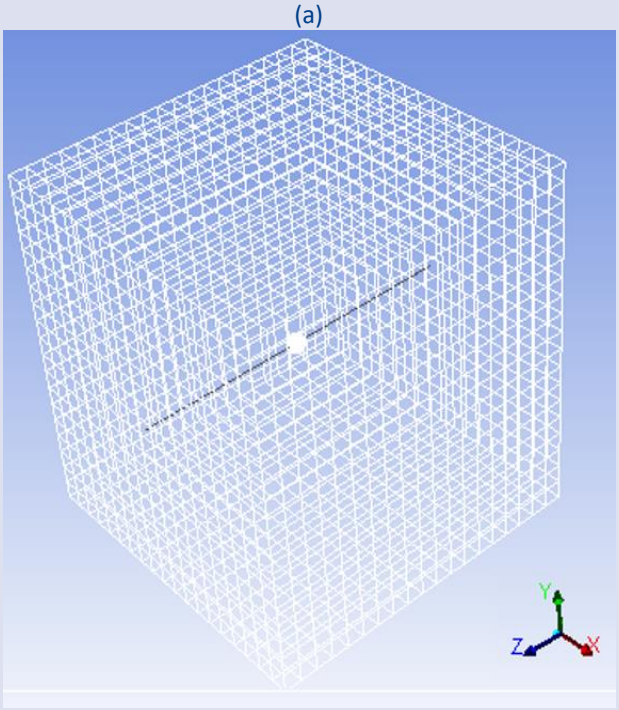

(b)

Figure 8. (A) Illustration of the plane, which is attached to the cancer cell. The plane cuts the cancer cell at the center. (B) The line, created from one side of the box to the other, cuts through the cancer cell.

In Figure 8(a), the plane attached to the cancer cell is black, and the cancer cell is white in the middle of the plane. The line can be seen in Figure 8 (b)—both the plane and the line cut through the cancer cell.

After creating planes very close to the cancer cell, the heat effect is analyzed on the cancer cell and the healthy tissues surrounding it. The change of temperature on the cancer cell and the cut plane (Figure 9) is shown in Figure 9.

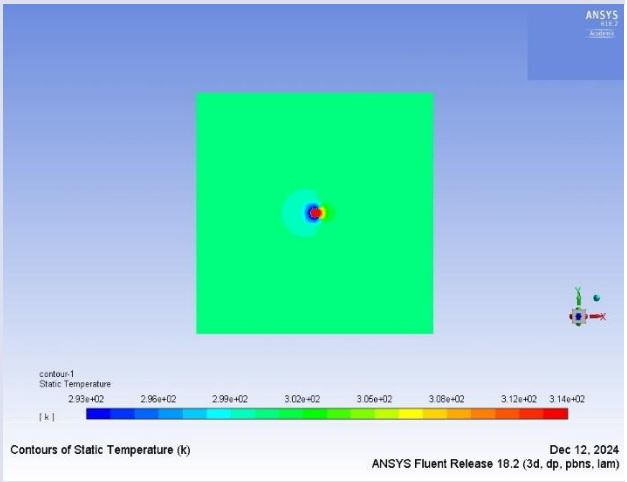

Figure 9. Contours of temperature both on the cancer cell and the healthy tissue near the cancer cell.

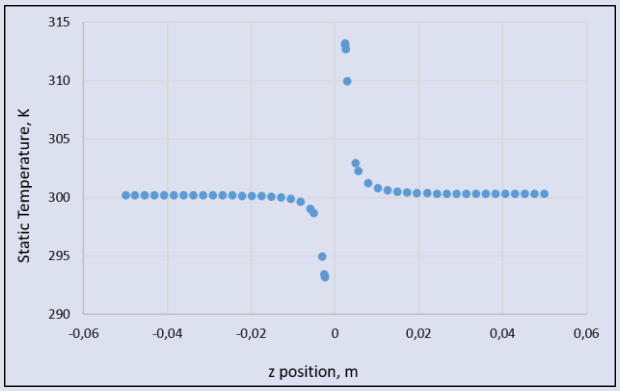

Figure 10. The temperature changes on the healthy tissue near the cancer cell.

The heat effect during photothermal therapy is essential for the healthy cells around the sick cell. As seen in Figure 10, the temperature in the healthy tissues, which are very close to the cancer cell, is mostly around 300 K. Moreover, the temperature is lower in the colder part of the cancer cell, which is about 298 K. The temperature effect on the line (shown in Figure 8) can be seen in Figure 10. The cancer cell is in the middle, where the temperature goes up and down in Figure 10.

After analyzing the temperature changes, the pressure variations on the healthy tissues around the cancer cell are also determined (Figure 11).

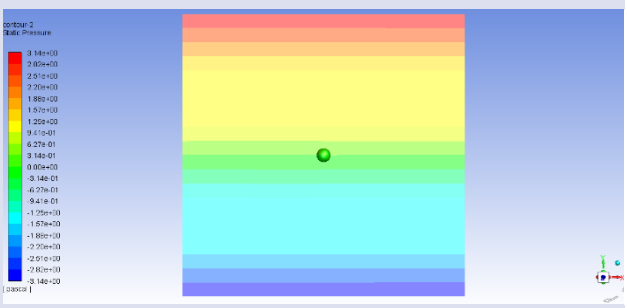

Figure 11. Pressure contours the healthy tissue near the cancer cell.

As discussed in part 3.1, the pressure effect in the cancer cell and its vicinity is essential for changing its behavior [25]–[28]. As shown in Figure 11, the pressure values of healthy tissue around the cancer cell increase away from the cancer cell. Providing a quantitative validation for the CFD model is currently not available because of the deficiency of the experimental data.

Conclusion

For a deadly illness, there have been alternative therapies for cancer treatment, such as photothermal therapy. However, it is necessary to know that the heat distribution is suitable and that the surrounding tissue is not overheated. This work models the cancer cells and the surrounding healthy tissue using CFD. The temperature distribution of cancer cells and the healthy tissue is examined. Current findings show that temperature changes occur very near the cancer cell. Moreover, the cancer cell and the healthy tissue pressure are also affected by the PTT of cancer cells. The wall shear stress profile also affects the stiffness and adhesion of cancer cells to the microvasculature. Overall, this study concludes that the cancer cell and the tissue around it can be modeled effectively by using CFD. It has been shown that when photothermal therapy is used, the healthy tissue around the cancer cell is unaffected, demonstrating photothermal therapy's effectiveness. The results of this work could guide researchers in optimizing the photothermal therapy of cancer cells, and the modeling approach could be applied to investigate alternative therapies.

Conflicts of interest

There are no conflicts of interest in this work.

References

[1] Ferlay J., Ervik M., Lam F., Colombet M., Mery L., Pineros M., Global Cancer Observatory: Cancer Today. Lyon: International Agency for Research on Cancer. https://gco.iarc.fr/today. Retrieved July, 2024.

[2] Gong F., Liu J., Yang J., Qin J., et al., Effective Thermal Transport Properties in Multiphase Biological Systems Containing Carbon Nanomaterials, *RSC Adv*., 7(22) (2017) 13615–13622.

[3] Cherukula K., Manickavasagam Lekshmi K., Uthaman S., Cho K., Cho C-S., Park I-K., Multifunctional Inorganic Nanoparticles: Recent Progress in Thermal Therapy and Imaging, *Nanomater*, 6(4) (2016) 76.

[4] Yang K., Feng L., and Liu Z., Stimuli responsive drug delivery systems based on nano-graphene for cancer therapy, *Adv. Drug Deliv. Rev*., 105 (2016) 228–241.

[5] Cherukuri P., Glazer E.S., Curley S.A., Targeted hyperthermia using metal nanoparticles, *Adv. Drug Deliv. Rev*., 62(3) (2010) 339–345.

[6] Manthe R. L., Foy S. P., Krishnamurthy N., Sharma B., Labhasetwar V., Tumor Ablation and Nanotechnology, *Mol. Pharm.*, 7(6) (2010) 1880–1898.

[7] Lal S., Clare S.E., Halas NJ., Nanoshell-Enabled Photothermal Cancer Therapy: Impending Clinical Impact, *Acc. Chem. Res*., 41(12) (2008) 1842–1851.

[8] Robinson J.T., Tabakman S.M., Liang Y., Wang H., et al., Ultrasmall Reduced Graphene Oxide with High Near-Infrared Absorbance For Photothermal Therapy, *J. Am. Chem. Soc*., 133(17) (2011) 6825–6831.

[9] Liu H., Chen D., Li L., Liu T., et al., Multifunctional Gold Nanoshells On Silica Nanorattles: A Platform for the Combination Of Photothermal Therapy And Chemotherapy With Low Systemic Toxicity, *Angew. Chem. Int. Ed. Engl*., 50(4) (2011) 891–895.

[10] Cheng L., Yang K., Chen Q., Liu Z., Organic stealth nanoparticles for highly effective in vivo near-infrared photothermal therapy of cancer, *ACS Nano*, 6(6) (2012) 5605–5613.

[11] van der Zee J., Heating the Patient: A Promising Approach?, *Ann. Oncol. Off. J. Eur. Soc. Med. Oncol*., 13(8) (2002) 1173–1184.

[12] Dahl O., Interaction of Heat and Drugs in Vitro and in Vivo. In: Seegenschmiedt M.H., Fessenden P., Vernon C.C., (Eds.). Thermoradiotherapy and Thermochemotherapy: Biology, Physiology, Physics. Springer, Berlin Heidelberg, (1995) 103–121.

[13] Gonzalez D.G., van Dijk J.D.P., Blank L.E.C.M., Rümke P., Combined Treatment With Radiation And Hyperthermia Inmetastatic Malignant Melanoma, *Radiother. Oncol*., 6(2) (1986) 105–113.

[14] Kim J. H., Hahn E. Tokita W., N., Nisce L. Z., Local Tumor Hyperthermia in Combination with Radiation Therapy. 1. Malignant Cutaneous Lesions, *Cancer*, 40(1) (1977) 161–169.

[15] Coleman A., Augustine C. K., Beasley G., Sanders G., Tyler D., Optimizing Regional Infusion Treatment Strategies for Melanoma of the Extremities, *Expert Rev. Anticancer Ther*.,9(11) (2009) 1599–1609.

[16] Kamarudin S., Taib I., Adnan M., Nasir F., et al., Prediction of Heat Distribution on Brain Malignant Tumor Using Hyperthermia Therapy, *AIP Conf. Proc*., 2955(1) (2023). 20031.

[17] Haar L., Gallagher J.S., Kell G.S., NBS/NRC steam tables: thermodynamic and transport properties and computer programs for vapor and liquid states of water in SI units. Washington (DC) Hemisphere, (1984).

[18] Marsh K.N., Recommended reference materials for the realization of physicochemical properties. Blackwell Scientific Publications, (1987).

[19] Sengers J.V., Watson J.T.R., Improved International Formulations for the Viscosity and Thermal Conductivity of Water Substance, *J. Phys. Chem. Ref. Data*, 15(4) (1986) 1291–1314.

[20] Archer D.G., Wang P., The Dielectric Constant of Water and Debye-Hückel Limiting Law Slopes, *J. Phys. Chem. Ref. Data*, 19(2) (1990) 371–411.

[21] Vargaftik N. B., Volkov B. N., Voljak L. D., International Tables of the Surface Tension of Water, *J. Phys. Chem. Ref. Data*,12(3) (1983) 817–820.

[22] Dabagh M. Randles A., Role of Deformable Cancer Cells on Wall Shear Stress-Associated-VEGF Secretion by Endothelium in Microvasculature, *PLoS One*, 14(2) (2019) e0211418.

[23] Basson M.D., Zeng B., Downey C., Sirivelu M.P., Tepe J.J., Increased Extracellular Pressure Stimulates Tumor Proliferation by A Mechanosensitive Calcium Channel and PKC-β, *Mol. Oncol.,* 9(2) (2015) 513–526.

[24] Ingber D.E., Can Cancer Be Reversed by Engineering the Tumor Microenvironment?, *Semin. Cancer Biol.,*18(5) (2008) 356–364.

[25] Gutmann R., Leunig M., Feyh J., Goeat A.E., et al., Interstitial Hypertension in Head and Neck Tumors in Patients: Correlation with Tumor Size, *Cancer Res.,*52(7) (1992) 1993–1995.

[26] Raju B., Haug S. R., Ibrahim S. O., Heyeraas K. J., High Interstitial Fluid Pressure in Rat Tongue Cancer is Related to Increased Lymph Vessel Area, Tumor Size, Invasiveness and Decreased Body Weight, J. Oral Pathol. Med., 37(3) (2008) 137–144